Key Points:
- Distinct fresh features are observed within the subtropical North Atlantic
- Mesoscale turbulence is significant in governing the surface salinity

Correspondence to:
J. Busecke,
julius@ldeo.columbia.edu

Subtropical surface layer salinity budget and the role of mesoscale turbulence

Julius Busecke[1], Arnold L. Gordon[1], Zhijin Li[2], Frederick M. Bingham[3], and Jordi Font[4]

[1]Lamont-Doherty Earth Observatory of Columbia University, Palisades, New York, USA, [2]Jet Propulsion Laboratory, California Institute of Technology, Pasadena, California, USA, [3]Center for Marine Science, University of North Carolina Wilmington, Wilmington, North Carolina, USA, [4]SMOS Barcelona Expert Centre (SMOS-BEC), Institut de Ciencies del Mar CSIC, Barcelona, Spain

Abstract The subtropical North Atlantic exhibits the saltiest surface waters of the open ocean. Eventually that water subducted from the surface and exported toward the Equator, as a subsurface salinity maximum (S-max) forming the lower limb of the subtropical cell. Climatologically, the winter subtropical surface water, coinciding with the deepest mixed layer of ∼100 m, is saltier and colder than the S-max. Towed CTD measurements in March/April 2013 (a component of the field program SPURS) within the North Atlantic subtropical surface salinity maximum reveal several relatively fresh, warm anomalies, which deviate strongly from climatological conditions. These features introduce a large amount of freshwater into the subtropical region, exceeding the amount introduced by local rain events. Observed scales and evolution of the features strongly suggest a connection to mesoscale dynamics. This is supported by high-resolution regional model output, which produces an abundance of features that are similar in scale and structure to those observed. It is hypothesized that turbulent transport in the surface ocean is a crucial process for setting mixed layer characteristics, which spread into S-max stratum. High variability in the EKE implies a high potential for interannual variability in the resulting S-max water properties by ocean dynamics in addition to the variability caused by air sea fluxes. This has likely consequences to the meridional transport of heat and freshwater of the subtropical cell in the North Atlantic and to the larger-scale ocean and climate system.

1. Introduction

The response of the global freshwater cycle to a changing climate is certainly one of the most pressing questions to answer in order to anticipate and adapt to global climate change [*Schmitt*, 2008]. The ocean is the key element in the global water cycle. It contains about 97% of the Earths free water and accounts globally for 86% of the evaporation and 78% of the precipitation [*Schmitt*, 1995]. Understanding the marine hydrological cycle is thus crucial to improve the understanding of the global water cycle, including the implications for the terrestrial water cycle. Sea surface salinity (SSS) is an indicator of the marine hydrological cycle, but it is not as straightforward as a rain gauge on land, as advection and mixing (horizontally and vertically) within the ocean can also alter the salinity. To interpret changes in the freshwater cycle using the SSS, it is necessary to understand the underlying ocean processes in order to piece together a full picture of the hydrological cycle in the ocean and its coupling to the atmosphere.

The horizontal SSS maximum (SSS-max) in the subtropical North Atlantic has the highest open-ocean values of SSS in the world. The region of the SSS-max (centered near 25N, 38W; Figure 1a) is highly evaporative [*Schanze et al.*, 2010], with evaporation exceeding precipitation (E– P > 0) the entire year. To balance this loss, fresher waters have to be advected or mixed both horizontally and vertically into the salty surface layer. Salty surface waters are exported equatorward below the surface, forming the S-max core near 100–150 m [*Worthington*, 1976], often referred to as the subtropical underwater [*O'Connor et al.*, 2005]. In the tropics, wind-induced Ekman divergence causes upwelling of the subsurface waters, which are subsequently freshened due to excess rainfall. On average Ekman transport spreads the lower salinity surface water toward the subtropics, closing the shallow overturning cell [*Schott et al.*, 2004]. This manuscript will use the equivalent but more widely used term subtropical cell (STC). The STC has been described as a major ocean circulation feature which is important to the poleward heat transport [*Boccaletti et al.*, 2005], and as such is important for the global climate.
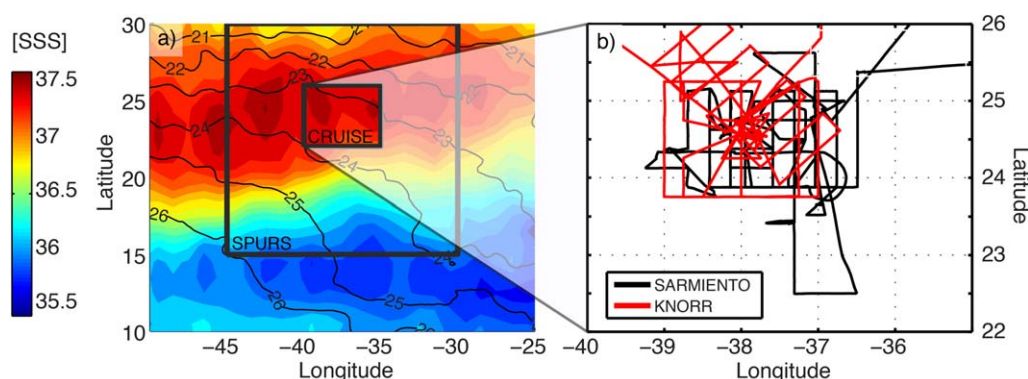
Figure 1. (a) Sea surface salinity (PSU) from Aquarius L3 (V2) in color and sea surface temperature (°C) from NOAA OISST V2 in black contours, averaged for March and April 2013. The black boxes indicate the domains used in the text. (b) Cruise tracks for the two research vessels utilized in this study. The cruises took place between 2012 and 2013: KNORR (September–October 2012) and SARMIENTO (March–April 2013).

The climatological SSS-max is depicted as a region with low lateral gradients of salinity, due to data averaging and smoothing procedures [e.g., *Schmitt*, 2008, Figure 1b]. Using underway data from research and commercial vessels [*Reverdin et al.*, 2007], and now the Aquarius (F. M. Bingham et al., 2014, The north atlantic subtropical surface salinity maximum as observed 522 by aquarius, under review in *Journal of Geophysical Research: Oceans*) and SMOS [*Font et al.*, 2010] satellites, the SSS field can be observed at much higher resolution than before, revealing far more variability, with a robust seasonal cycle and shifts in position of the SSS-max. Net evaporation and surface salinity are anticorrelated [*Gordon and Giulivi*, 2014] and the maximum surface salinity is located north of the E-P maximum [e.g., *Schmitt*, 2008], both strong indications of the significant influence of oceanic processes in setting the water properties and controlling the variability of the SSS-max.

The ocean processes responsible for controlling mixed layer properties in the SSS-max and the export of salty surface waters into the S-max layer are the subject of this study, with a focus on the influence of turbulent mesoscale structures in the surface layer that stir freshwater into the region, as observed during the SPURS (Salinity Processes in the Upper Ocean Regional Study; http://spurs.jpl.nasa.gov) field project.

2. Data and Methods

Most of the data described herein were collected during one of the field expeditions organized within the SPURS project. The measurements were carried out between March 22nd and April 8th on the Spanish research vessel SARMIENTO DE GAMBOA (SPURS-MIDAS cruise, track shown in Figure 1b). Additional data sets used in this study are listed below. Throughout the text, the CRUISE-domain and SPURS-domain (Figure 1a) will be used for spatial reference.

2.1. Underway

The underway thermosalinograph (TSG, model SeaBird SBE 21) was located at 2–3 m depth near the bow of the ship, measuring temperature and conductivity in 6 s intervals. The TSG data showed periods of very high variability, which might be caused by several reasons like the shallow intake entraining bubbles due to ship movement, variable flow rates in the seawater system, or strong diurnal warming and salinification, leading to strong gradients in the upper meters of the water column, as indicated by other measurements during previous cruises. All data shown are smoothed with a Gaussian window of 20 min length. The salinity calibration was performed by adjusting to water samples drawn from the seawater system. A constant value is fitted to the residuals between the TSG and water samples weighted by the normalized inverse of the variance that was experienced within ∼4 min before the sample was taken. This method reduces the error due to uncertainty in the transit time from TSG to the sample station. The estimated constant offset that was determined this way is 0.04 PSU. The temperature data were adjusted by preselecting samples with wind speed > 8 m/s and during nighttime, which have been seen to exhibit very small vertical gradients in the upper meters within this region (D. Fratantoni, personal communication). The temperature was then adjusted downward by a constant offset such that 99% of the samples are neutral or stably stratified (comparing the TSG and SeaSoar). This yields an offset of 0.59 °C. Since the temperature is not determined by a

hull sensor, but rather after the water passes through the intake pump, the bias could be due to the influence of the ship and pump, which might vary over time and with the flow rate.

2.2. Shipboard Acoustic Doppler Current Profiler (SADCP)

The shipboard instantaneous velocities were recorded by a Teledyne RDI 75 Khz Workhorse Ocean Surveyor. Due to low scatter environments, the narrow band mode and a bin size of 16 m was chosen (the topmost bin was centered at ∼24 m). The data presented in this study were averaged to 2 min intervals.

2.3. SeaSoar

The SeaSoar towed sensor system was equipped with dual pumped temperature/conductivity sensors. A final calibration is not available as of now. Initial comparison between sensors yields differences that are at least an order of magnitude lower than the gradients of structures relevant to this study and should not significantly bias our findings. SeaSoar data were averaged on 1 dbar bins and over 10 min intervals, ensuring that the full cycle from bottom to surface of the SeaSoar is included in every binned profile. Figure 2 shows examples of the along track variability and typical vertical profiles that were recorded by the SeaSoar. There is large variability in potential temperature, salinity, and density, representing strong active fronts in the mixed layer, as temperature and salinity are not compensated in density over various regions of the record.

2.4. CTD

Additional subsurface data from the KNORR cruise in September/October 2012 are used for a seasonal comparison (see Discussion). 99 CTD profiles were collected in the measurement area (cruise track is shown in Figure 1b).

2.5. MIMOC climatology

The MIMOC climatology is a gridded seasonal climatology derived primarily from Argo data. It provides monthly profiles on a 0.5×0.5 deg grid [*Schmidtko et al.*, 2013] (V 2.2 on a z grid was used in this study). The data set is available at http://www.pmel.noaa.gov/mimoc/. Mixed layer depth was determined by a density difference to the surface exceeding 0.1 kg/m^3.

2.6. TRMM

For the analysis of rain event size in the region TRMM (Tropical Rainfall Measuring Mission) data (product: 3B42, http://mirador.gsfc.nasa.gov), with a spatial resolution of 1/4 degrees and temporal resolution of 3 h was used. Connected grid cells of > 1 mm/h rain rate within the SPURS area are indexed as individual rain events. The 1 mm threshold is chosen arbitrary, but results derived in this study do not significantly depend on the choice of the threshold value. For each event, the rain rate is multiplied by the time resolution and summed over time and space, yielding the total volume of freshwater that enters the ocean. Additionally, the mean rain rate and duration of each event were calculated.

2.7. AVISO

For the assessment of the spatial structure of surface velocities, AVISO altimeter data are used. The product (dt_upd_global_merged_msla_uv, October 1992 to July 2013, http://www.aviso.oceanobs.com) is treated as geostrophic zonal and meridional velocity anomalies u and v with respect to a long-term mean. These are decomposed into $u = \bar{u} + u'$ at each grid point using a 3 month Gaussian window, in order to separate seasonal and longer fluctuations ($\bar{u}$) from the mesoscale signal (u'). The Eddy Kinetic Energy (EKE) was calculated as: $EKE = 1/2((u')^2 + (v')^2)$.

2.8. ROMS

We set up a regional modeling system, based on the Regional Ocean Modeling System (ROMS) [*Shchepetkin and McWilliams*, 2009]. ROMS is configured as a nested set of three spatial domains, centered at 38W and 24.5N. The outside domain has a horizontal resolution of 9 km for a region of 2500 km by 2800 km, the next domain has a resolution of 3 km for a region of 1100 km by 1000 km, and the last domain has a resolution of 1 km for a region of 360 km by 300 km. There are 50 vertical levels with a resolution of a few meters near the surface. The lateral boundary condition is the climatology, consisting of the monthly means derived from the Hybrid Coordinate Ocean Model (HYCOM) outputs of 4 years, from September 2008 through August 2011. The HYCOM model uses a resolution of about 9 km and data assimilation. (http://hycom.org/dataserver/glb-analysis). One-way nesting is used for the lateral boundary condition for the two fine grid
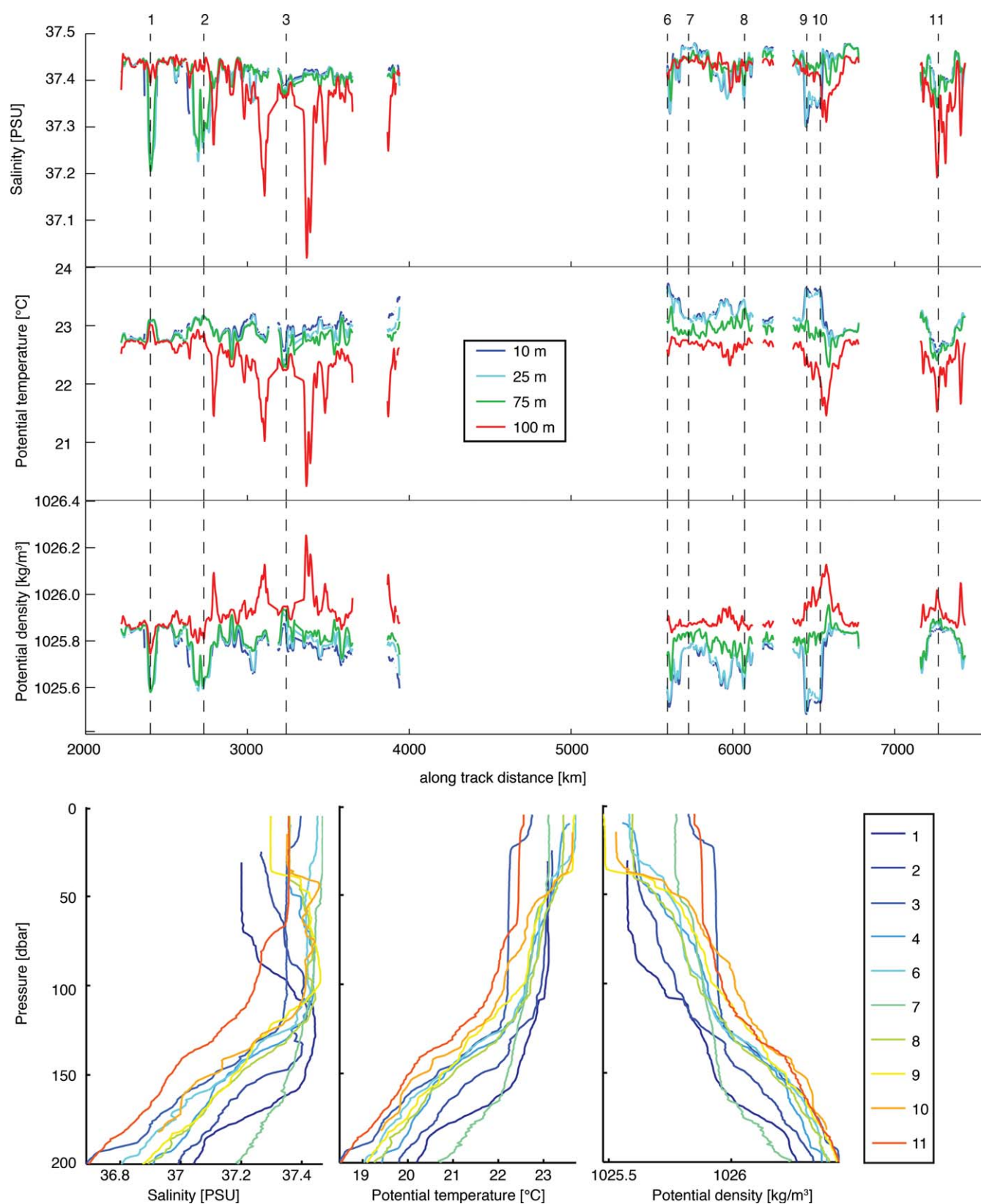
Figure 2. SeaSoar data. (top) Track variations of salinity (PSU)/potential temperature (°C)/density (kg/m³). A Gaussian window of 60 min length is used as a low pass filter for clarity in this figure. Depths are color-coded. Note that large excursions at 100 m depth are confined to that depth and hence represent depth variations of the permanent pycnocline rather then surface variability. (bottom) Typical profiles of salinity/potential temperature/density with depth. Line color corresponds to marker numbers for spatial reference during the survey (see top plot and other figures).

domains [*Blayo and Debreu*, 1999]. The results presented here are extracted from the domain with a resolution of 3 km. To compute the surface fluxes, the atmospheric fields of 10 m winds, 2 m temperatures, precipitation rates, humidity, short-, and long-wave radiation are used. They are derived form hourly forecasts from the Global Forecast System (GFS) at the National Center for Environmental Prediction (NCEP) and used to compute the wind stresses, evaporation, latent, and sensible heat fluxes.

2.9. Aquarius

Aquarius CAPv2.0 L3 weekly SSS data are used in this study. They are available at (ftp://podaac-ftp.jpl.nasa. gov/allData/aquarius/).

2.10. Budgets and Turbulent Flux Definitions

The aim of this study is to evaluate the influence of mesoscale turbulence to the salinity budget in the subtropical North Atlantic. The equilibrium mass balance is given by

$$\iiint_V \nabla \cdot \rho \vec{v}\, dV = \oiint_{A_i} \rho \vec{v} \cdot \vec{n}\, dA = \oiint_{A_s} F\, dA \tag{1}$$

A_i denotes the interior surface and A_s the sea surface area of an arbitrary volume V, ρ is the density and $\vec{v}$ the velocity vector. The forcing term F is the massflux at the surface (negative for evaporation), and $\vec{n}$ is the normal vector to the interior surface. When molecular diffusion and small-scale mixing are neglected, the equilibrium salt budget can be written as

$$\iiint_V \nabla \cdot \rho S \vec{v}\, dV = \oiint_{A_i} \rho S \vec{v} \cdot \vec{n}\, dA = 0 \tag{2}$$

For this study, changes in density are neglected and ρ is assumed constant. From the mass balance follows:

$$\bar{F} = \rho \frac{A_i}{A_s} \overline{\vec{v} \cdot \vec{n}} \tag{3}$$

Overbars denote time-averaged values. Similarly, the salt budget can be written as:

$$V[\overline{\nabla \cdot S\vec{v}}] = A_i \overline{S\vec{v} \cdot \vec{n}} \tag{4}$$

For the rest of this study, we will assume a simplified box volume: $V = A_s h$ where h is the depth of the box. Then, the volume flux of freshwater out of the surface can be related to a salinity divergence within the volume using a constant reference salinity S_0:

$$\overline{F_V} = \frac{\bar{F}}{\rho} = -\frac{h}{S_0}[\overline{\nabla \cdot S\vec{v}}] \tag{5}$$

Note that this is an average flux over a surface area of $A_s = 1$ m^2. A similar formulation can be used to calculate the absolute volume of freshwater V_{FW} that must be added to a volume of water with salinity S_1 to produce a box volume of depth h, surface area $A_s = 1$ m^2 and salinity S_2:

$$V_{FW} = \frac{h}{S_0}(S_1 - S_2) \tag{6}$$

We now decompose the velocity and salinity into slowly varying mean fluxes (denoted by overbars) and turbulent (eddy) fluxes (time fluctuations shorter than 3 months, denoted by prime terms). This yields the following for the salinity flux term in equation (5):

$$\overline{S\vec{v}} = \bar{S}\,\overline{\vec{v}} + \overline{S'\vec{v}'}. \tag{7}$$

This study will focus on the turbulent salinity flux out of the SSS-max area (the second term on the rhs). For simplicity, the term "equivalent freshwater flux" will be used throughout the manuscript, noting that mass

cannot be mixed and we are dealing with a turbulent salinity flux which can be expressed as equivalent freshwater flux of opposite sign, using equations (5) and (7):

$$\overline{F_V} = -\frac{h}{S_0}[\nabla \cdot \overline{S'\vec{v'}}] = -\frac{h}{S_0}[\nabla \cdot \overline{K\nabla S}] \qquad (8)$$

The turbulent salinity flux $\overline{S'\vec{v'}}$ is approximated here by the product of a surface eddy diffusivity K and the gradient of the slowly varying mean surface salinity field. This simplified formalism enables easy comparison of the relative role of turbulent lateral salinity fluxes and surface freshwater (mass) forcing in the area.

3. Observations

The surveyed region showed large upper ocean variability in time and space and on a variety of scales (Figure 2), in agreement with earlier underway measurements within this region. The SeaSoar and TSG surveys (Figure 3) revealed several distinct features in the surface layer above the permanent pycnocline. Areas of deep mixed layers (up to 150 m), penetrating to the pycnocline were generally found to be the saltiest waters in the region with a salinity of ∼37.4 *PSU* and higher. These waters agree well with the climatological surface values in this region for March and April as well as the average properties in the upper 50 m over the whole cruise (compare the MIMOC profiles for March/April and the lower black diamond in Figure 4). These waters are subsequently referred to as SSS-max waters. The temperature and salinity (T/S) measurements show a considerable spread but there are two categories of water characteristics that deviate significantly from the SSS-max waters. Two principal types of fresh features, with higher and lower temperature than the SSS-max water, were found and their importance to the SSS-max region will be investigated below.

3.1. Warm/Fresh Features

The first warm and fresh feature was observed between ∼37.75W−36.5W and 23.75N−24.5N (Figures 3a and 3b, markers 1 and 2). Initially this feature had a strong surface signature in temperature/salinity/density with pronounced surface and subsurface fronts to the east and slightly weaker fronts to the west. Changes in surface properties reach values on the order of 0.2 PSU and 0.3 °C over distances on the order of 10 km (Figure 5 upper panel). Water properties from near-surface TSG and deeper SeaSoar measurements compare well within the fresh feature. The fresh water defines a new mixed layer now considerably shallower (less than 90 m; e.g., Figure 5) than the surrounding SSS-max mixed layer. Below, the stratification between the base of the mixed layer and the permanent pycnocline is weak, and properties match the surrounding SSS-max waters which are colder and saltier. The surface fields in survey 2 (Figures 3c and 3d) show a warm and fresh anomaly with an increased surface area extending further to the north (see Figure 3c black arrows). The northwestern extent of the fresh water is sampled well by cruise pattern and is found to the north of the location of the feature in survey 1, suggesting a northward advection of the fresh water volume (This will be supported by the AVISO/ADCP velocities discussed below). Surface gradients appear to be reduced compared to the first survey. The third survey (Figures 3e and 3f) shows only filamented structures with spatial extent of less than 25 km (Figure 3 markers 6 and 8). This discussion assumes that the fresh/warm anomaly at the surface is, at least in surveys 1 and 2, one coherent structure. Given the high spatial and temporal variability along the ship track and missing subsurface data in survey 2, this assumption cannot be conclusively proven (Figures 3c and 3d). Yet the TSG can be used with confidence to identify the extent of the anomaly, which along with the upper ocean velocity field described below, enable us to speculate on the movement of the fresh anomaly within the domain.

The final survey (Figures 3g and 3h) was carried out to extend the survey southward where AVISO altimetry data and ROMS model output (not shown), reveal large EKE and surface salinity gradients, implying the potential for large eddy fluxes, which may be the ocean process shaping the annual cycle of the SSS-max and ultimately the S-max. Toward the south in survey 4 (Figures 3g and 3h), there is an anomaly similar to the one discussed above, again with a pronounced surface gradient (see markers 9 and 10). This warm, fresh feature forms a strong lateral front with shallower mixed layers within the fresh area and the water below matching the adjacent deep SSS-max mixed layer waters (Figure 5). The temperature difference across the front is even slightly higher compared to the feature in survey 1 (up to 0.5 °C and 0.15 PSU over
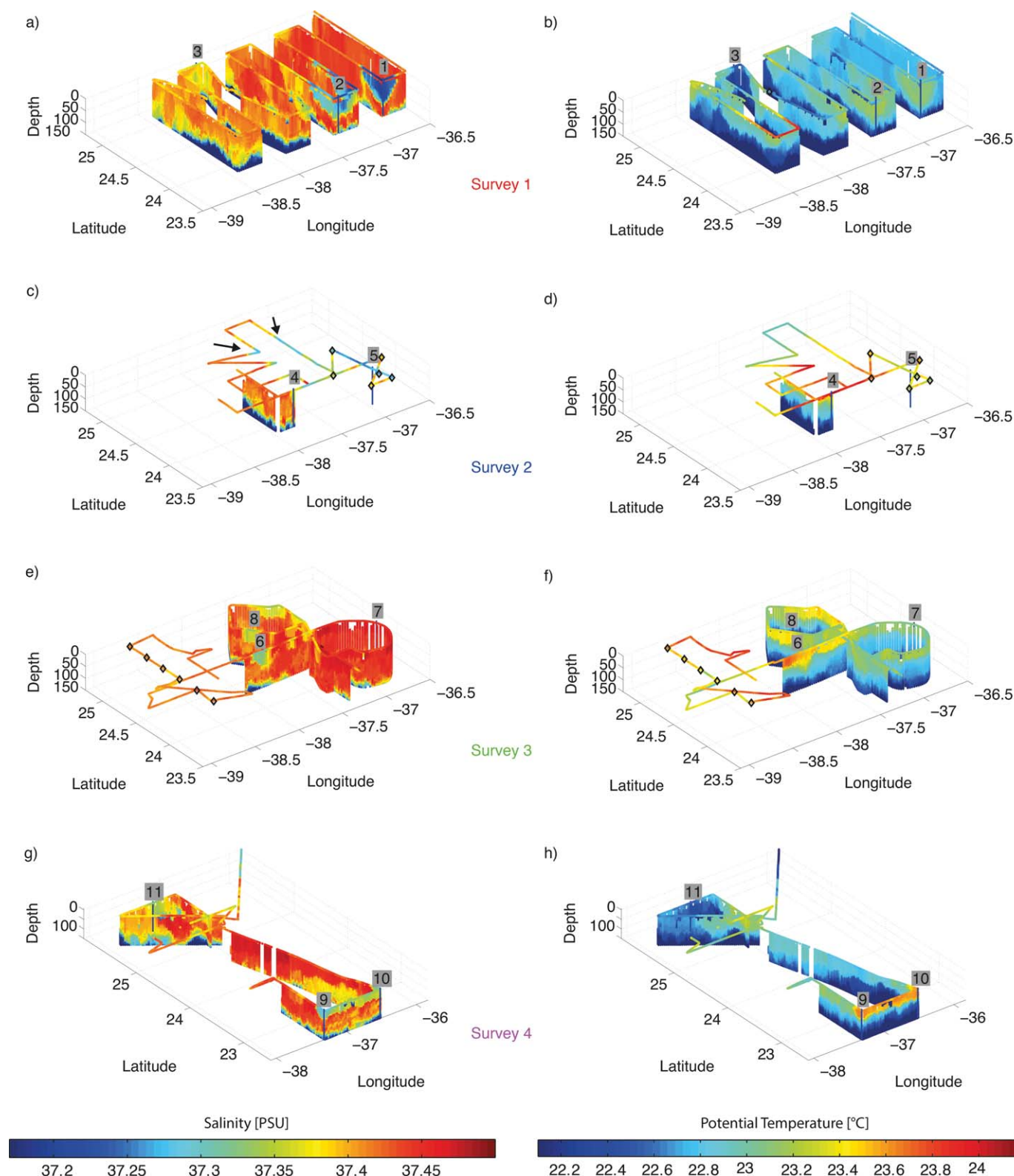
Figure 3. SeaSoar and TSG surveys. (left column) Salinity (PSU). (right column) Potential temperature (°C) (top row) 22–28 March; (second row) 28–31 March; (third row) 31 March to 4 April; (fourth row) 4–8 April. Numbers are time marker for cross-referencing between figures used throughout the manuscript. Black diamonds indicate CTD stations. Note the changed lateral scales for survey 4.
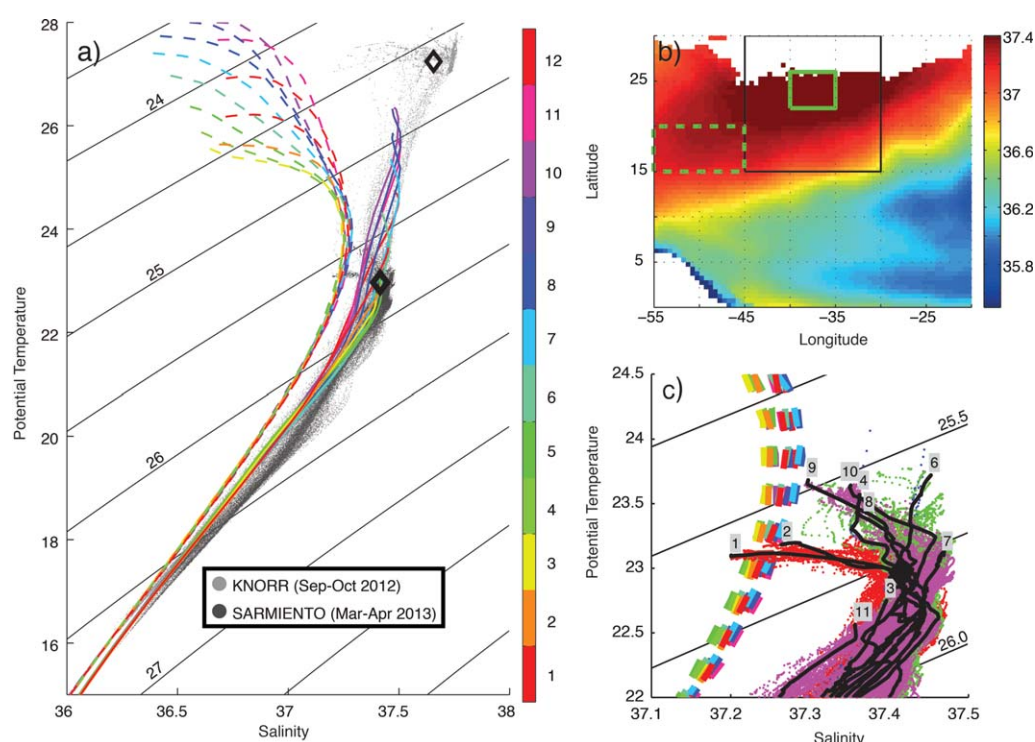
Figure 4. (a) θ (°C)/S (PSU) relation. Dots are SPURS cruises, dark gray for the SARMIENTO, and light gray for the KNORR. Dashed (solid) lines are from the MIMOC climatology and represent the region denoted by the dashed (solid) green box in Figure 4(b). Black diamonds are the upper 50 m average for each cruise, upper KNORR, lower SARMIENTO. Black contours show σ_0 density anomaly values (kg/m^3). (b) Annual average salinity (PSU) of the subsurface maximum from MIMOC. Large black box is the SPURS-domain. Green boxes describe areas for Figure 4a. (c) Dots: θ/S relation from Sarmiento SeaSoar. Survey 1 in red, survey 2 in blue, survey 3 in green, and survey 4 in violet. Thick black lines: Profiles of numbered marked locations. Refer to Figure 3 for survey numbers and marked locations. Thin black contours as in Figure 4a. Color-coded dashed lines are MIMOC θ/S relation from the Figure 4b green-dashed box.

distances of $\sim$ 10 km). This second patch extends roughly about 100 km in longitude, but an areal estimate is not precise, due to the limited pattern coverage close to the frontal region. The depth of the fresh mixed layer is slightly less than seen in the first feature. The evolution of this feature could not be observed during the cruise but its presence suggests that the phenomenon observed in the first survey is a regular occurring feature of this area.

3.2. Cold Features

Two cold subsurface anomalies were recorded during the cruise (Figures 3a and 3b marker 3 and Figures 3g and 3h marker 11). These features are fresher than the SSS-max water, but less so than the aforementioned warm features. They stand out mostly because they have a lower temperature than all of the surrounding mixed layer/deep mixed layer/surface waters. These features tend to have a very weak surface signature and generally show a stronger T/S structure below the surface. The T/S characteristics of these anomalies fit into the thermocline of this area (marker 3 and 11 in Figures 3a, 3b, 3g and 3h and Figure 4c), and they generally extend from the surface to the depth of the permanent pycnocline. Since the data do not enable us to analyze the evolution of one of those events as with the warm/fresh features, the behavior remains speculative. Compared to the warm fresh features, these were found further to the north in the measurement region in both observed cases. Rapid transects that include the northern part of the SPURS-domain include multiple fresh features within the mixed layer that show similar properties during the month of April [*Gordon and Giulivi*, 2014], indicating that these features might also be a regular phenomenon toward the northern boundary of the SSS-max.

3.3. The Fresh Columns

An interesting aspect of the fresh and warm feature in survey 1 is the structure directly adjacent to the mixed layer front. A fresh vertical column extends downward close to the strongly tilted isopycnals of the front (north of marker 1 in Figures 3a and 3b indicated by a black arrow in Figure 5 survey 1). Close to
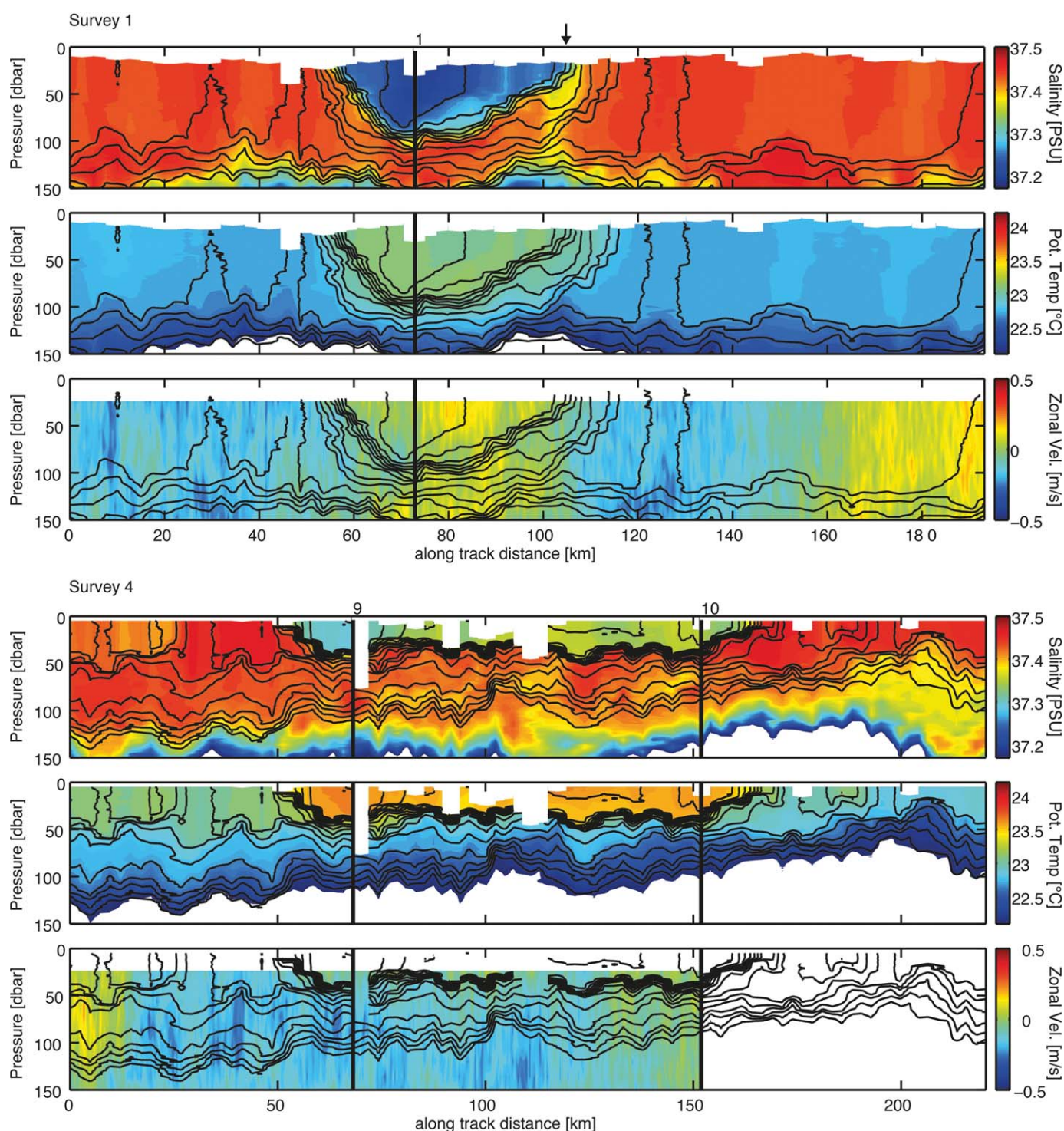
Figure 5. Section view of fresh features. The top three plots are taken from survey 1 (salinity (PSU) on the top, potential temperature (°C) on the mid, and zonal velocity (m/s) in the bottom plot). Black arrow indicates the position of the fresh column mentioned in the text. The three plots below are the same but for survey 4. Black vertical lines and numbers denote markers to provide spatial reference (see Figures 3a, 3b, 3g, and 3h). Black contours indicate potential density (interval: 0.03 kg/m³). Missing velocity data at the end of survey 4 was caused by an error in the ship motion sensors.

the surface isopycnals dip downward, possibly indicating negative vertical velocities on the heavier side of the front. This agrees qualitatively with the circulation across a strengthening horizontal mixed layer density front [*Klein and Lapeyre*, 2009] and the subsequent slumping collapse of the front
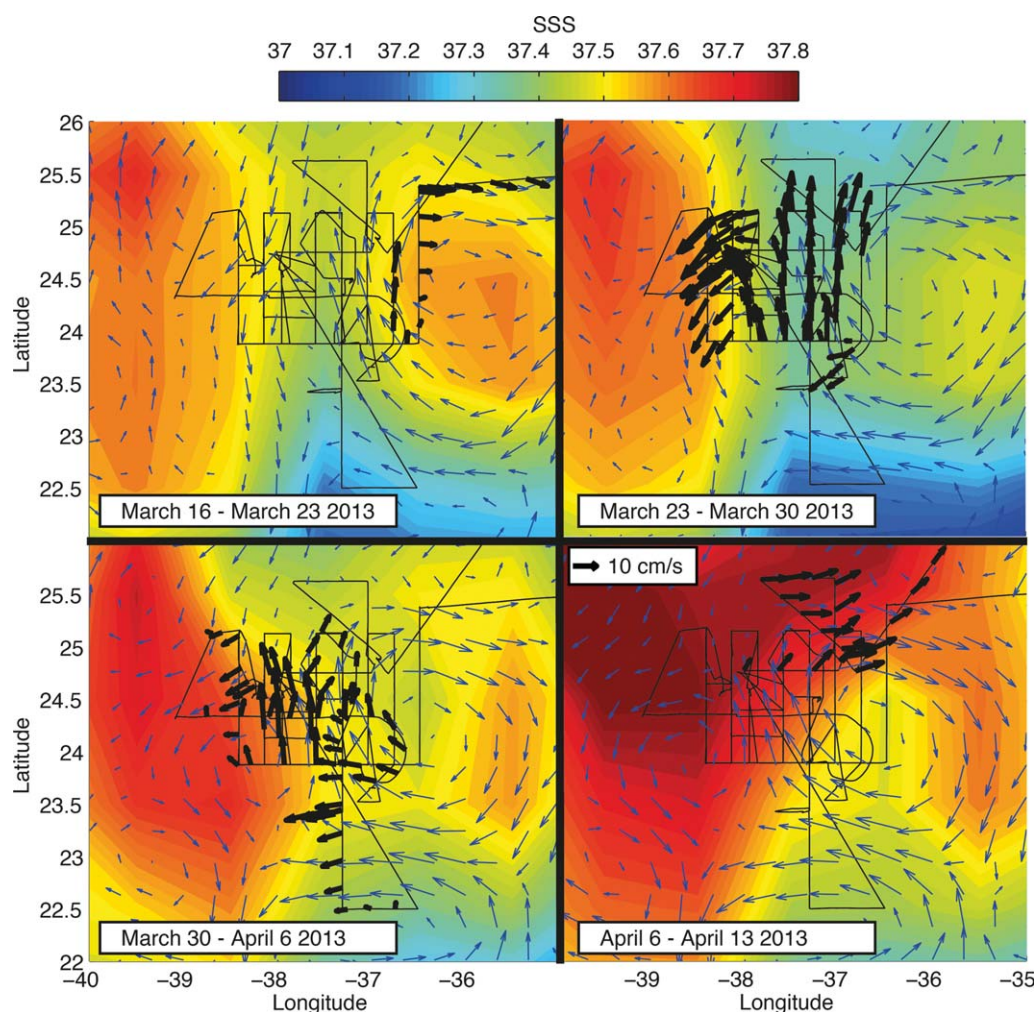
Figure 6. Black arrows: SADCP upper ocean velocities (20–100 m depth) measured from the SARMIENTO. The thin black line is the cruise track. Velocities are 1day-lowpass filtered and subsampled every 60th point, corresponding to a time resolution of 2 h. Blue arrows: Geostrophic velocities from AVISO altimetry. SSS from Aquarius is shown in color. Different plots depict different date ranges as shown in the lower left insets.

[e.g., *Fox-Kemper et al.*, 2008, Figure 2b]. If actually caused by vertical velocities, the downdrafts of fresh and warm water could act as a mechanism to freshen the underlying waters, which show weak stratification with depth and match the surrounding SSS-max mixed layers. This would imply that the fresh features and the associated dynamics at the mixed layer front could be vital in determining the water characteristics in the region, maybe even in the deeper layers above the pycnocline. The shipboard measurements only provide a snapshot section of salinity, which could be the result of vertical velocities induced by a submeso-scale ageostrophic circulation, or just the salinity signature of mesoscale stirring. Therefore, without additional data and analysis any conclusion drawn from this sample is highly speculative.

3.4. Upper Ocean Velocities

The upper ocean velocities inferred from altimetry measurements agree well with the shipboard velocity measurements averaged over the upper 100 m of the water column and 1day-lowpass filtered (Figure 6). The northward advection of the fresh and warm feature is clearly supported by both the AVISO and SADCP velocity measurements. The good agreement between the purely geostrophic AVISO velocities, SADCP velocities, and the evolution of the surface and subsurface salinities in the domain is compelling evidence for the role that mesoscale dynamics play in the behavior of these features. The Aquarius L3 SSS broadly depicts larger bodies of fresh water in the north and especially the south of the measurement domain, which could be related to the fresh features during the survey. Aquarius spatial resolution and estimated

accuracy [*Lagerloef*, 2013] is barely enough to resolve texture in the small measurement area, and comparison with the measurements at any given time on the cruise track is not useful. Nonetheless, the bigger picture seems to fit with our hypothesized mechanism of fresh water intruding into the area from a larger body of fresh water to the south. The general structure of SSS seems to be aligned with some of the prominent velocity anomaly structures during the survey, which is an encouraging result for the Aquarius data, and promotes further use in the future.

4. Discussion

4.1. Importance for the Regional Salinity Budget

Following equation (6), the volume of freshwater needed to dilute SSS-max water of $S_1 = 37.4$ PSU to a typical value for the fresh feature of $S_2 = 37.2$ PSU yields $V_{FW} = 27$ cm $= 0.27$ m^3/m^2 (with $h = 50$ m as a typical depth for the fresh feature). Assuming a surface area with extent of a half circle with 50 km radius for the fresh feature gives a total volume of at least $V_{(FW,Total)} = 10^9$ m^3 for the anomaly. There are only three possible scenarios for the fate of this freshwater: advection, evaporation out of the surface, and mixing with the surrounding waters (both laterally and vertically).

First we will consider the possibility of lateral advection of the patch. The SeaSoar data suggest a northward advection in the south of the domain during survey 1 and 2, roughly in accordance to the AVISO velocities. To advect the southwestern edge in survey 2 following the AVISO fields to a region uncovered by measurements would imply unrealistic velocities well exceeding the previous movement of the feature as well as AVISO velocities. We conclude that the fresh structures sampled during survey 1–3 are indeed the same feature, hence we can speculate on the evolution of the feature. Obvious deformation of the fresh feature and weakening surface structures (discussed in detail later) further encourage the dismissal of the pure advection scenario. Additional comparisons with OSCAR current data (http://www.oscar.noaa.gov) were performed, which includes the effect of Ekman transport. Differences were marginal and not qualitatively different, hence we dismiss Ekman transport as an important factor for the advection of this specific feature.

The second possibility would be evaporation out of the surface. Earlier we estimated an additional 27 cm of fresh water that would need to evaporate out of every 50 m deep column with $A_s = 1$ m^2. The NCEP-GFS fields used for the ROMS simulation at the end of March indicate that evaporation is mostly between 0.5 and 3 m/yr. To remove the full amount of freshwater at this rate, it would take between 33 and 197 days, and with the April average net evaporation of 1.5 m/yr [*Gordon and Giulivi*, 2014] it would take 65 days. These estimates should be viewed as gross overestimations given that large-scale evaporation is not confined to the fresh surface waters: if strong evaporation is not perfectly aligned with the SSS, the relative salinity gradient between the salty and fresh water masses would be maintained, with both waters experiencing a corresponding increase in salinity. Since the temperature of the fresh and warm features is higher, we evaluated the influence of a synthetic imposed temperature difference on the evaporation, by using bulk formulae following *Fairall et al.* [1996]. The influence of the SST on the relative evaporation does not exceed 0.4 m/yr, resulting in an even longer time scale than 197 days for a pure evaporation scenario. Since the observed feature disappeared within about 14 days, we conclude that a substantial amount of the freshwater is added to the mixed layer budget in this area via mixing processes. A discussion of how the freshwater is dispersed this rapidly will be included below.

Given that a significant portion of the freshwater has to be added to the mixed layer in the SSS-max region, we need to evaluate the importance of this added freshwater for the SPURS-domain. Analyzing rain events, using the TRMM data set, shows that the volume of freshwater (hypothetically needed to produce the features) is larger than 98.5% of the accumulated freshwater volume of any single rain event in this area over the period from January 2009 to July 2013. The amount of freshwater carried within this structure might be even bigger due to the unknown southern extent of the anomaly. Here we have used accumulated freshwater volume, as outlined in the data and methods section, to account for a possible deformation of the rain-diluted water due to ocean dynamics. A more traditional approach, using the mean rain rate per event multiplied by the duration of each event leads to the same basic conclusion that less than 0.2% of the rain events add > 26 cm freshwater per m^2 to the ocean surface. Along with the previous conclusions about the

role of evaporation and advection, this points to the relative importance of the documented T/S anomalies on the surface layer salinity budget in the SSS-max region.

Naturally this leads to the question whether the phenomenon of the intruding fresh features is an exception or if these events happen regularly in the area, matching the idea of lateral turbulent salinity flux as a significant component of the mixed layer salinity budget in this region. Multiple data sources confirm the abundance of these fresh features within the area. VOS and TSG [*Gordon and Giulivi*, 2014] as well as Aquarius (F. M. Bingham et al., in review, 2014) and ROMS model output show fresh and warm signatures year round, suggesting that these features play a significant role in balancing the excess evaporation at the surface by supplying freshwater to the region.

4.2. Origin of the Anomalies

This leads us to the next question: Where is the freshwater originating from and what is the driving mechanism?

A local rain event and the advection of water from a region outside the SSS-max would be the only plausible scenarios. We showed earlier that the amount of freshwater represented by the anomaly exceeds most rain events within this area. Additionally, the TRMM data for the time of the cruise do not show any rain activity that could explain the amount of freshwater contained in the observed fresh features. This further dismisses the process of local rain as explanation for the observations. Aquarius L2/L3 data at the time of survey 1 suggests an extensive area of fresh water to the south of the ship track (e.g., Figure 6). Combining this evidence substantiates the idea of the feature originating from a larger body of water. Climatologic mixed layer waters with characteristics corresponding to the fresh features are found in the south/southeast of the measurement area, extending from 39W to 31W between 20N and 22N in March with slightly greater zonal and northern extent in April. Matching T/S characteristics are also found further to the west from the CRUISE-domain, still within the SPURS-domain. The map in Figure 7a shows regions in the surface layer that match the fresh and warm anomalies as well as the climatological S-max properties. The northward advection of the first fresh/warm feature suggests that it originated from the south of the measurement area. The fact that survey 4, which was carried out toward the south of the previous surveys, encountered a similar fresh structure further establishes the idea of the south/southeast being the source of fresh water features. The relative importance of the western region as origin of fresh water is hard to evaluate from the spatial and temporally limited survey that is presented herein, but the velocity patterns discussed above do not show evidence for freshwater import from the west. A similar analysis of the water properties yields an origin toward the north of the SSS-max for the cold/fresh anomalies, observed during the cruise (not shown).

Preliminary analysis of ROMS model output supports the proposed origin and fate of the fresh feature. The ROMS output presented here is able to reproduce the upper ocean structure in the SPURS-domain reasonably well. The model shows more fresh surface data points, but the maximum surface salinity and associated mixed layer depth is similar (exceeding 37.4 PSU and 100 m mixed layer depth). The model shows an abundance of fresh features that penetrate into the SSS-max water. Figure 8 shows an example of a fresh feature that penetrates from the southern region into the SSS-max waters. The fresh water at the eastern border reaches as far north as 24N with a salinity of ∼37.2 *PSU*. This is remarkably similar to the feature seen in survey 1 (Figure 3). The fresh feature advances northward, gets partially separated and increasingly filamented within ∼ 16 days. The SeaSoar data suggest the dispersal of the fresh features within ∼ 14 days (beginning of survey 1 to end of survey 3), comparable to the feature in the model output. The depth of the simulated feature rarely exceeds 80 m and is found at approximately 50 m on average, values that compare well with the two fresh features seen in the SeaSoar survey (Figure 5). For the model, the spatial scale of the surface pattern of salinity varies strongly during the evolution of the feature. In particular, scales vary from ∼100−40 km during the first days and decrease down to ∼ 10 km after 16 days, suggesting an initial advection by mesoscale dynamics. This implies that the ROMS model is successfully reproducing the hypothesized dynamics of the observed fresh features, which supports our previous conclusions. Further analyses of the SPURS region using ROMS will be explored in a separate manuscript.

4.3. Mechanism for the Salinity Flux

The last part of our discussion will evaluate dynamic mechanisms that could be responsible for the influx of freshwater into the region as well as the observed fast dispersal within the SSS-max. The observed
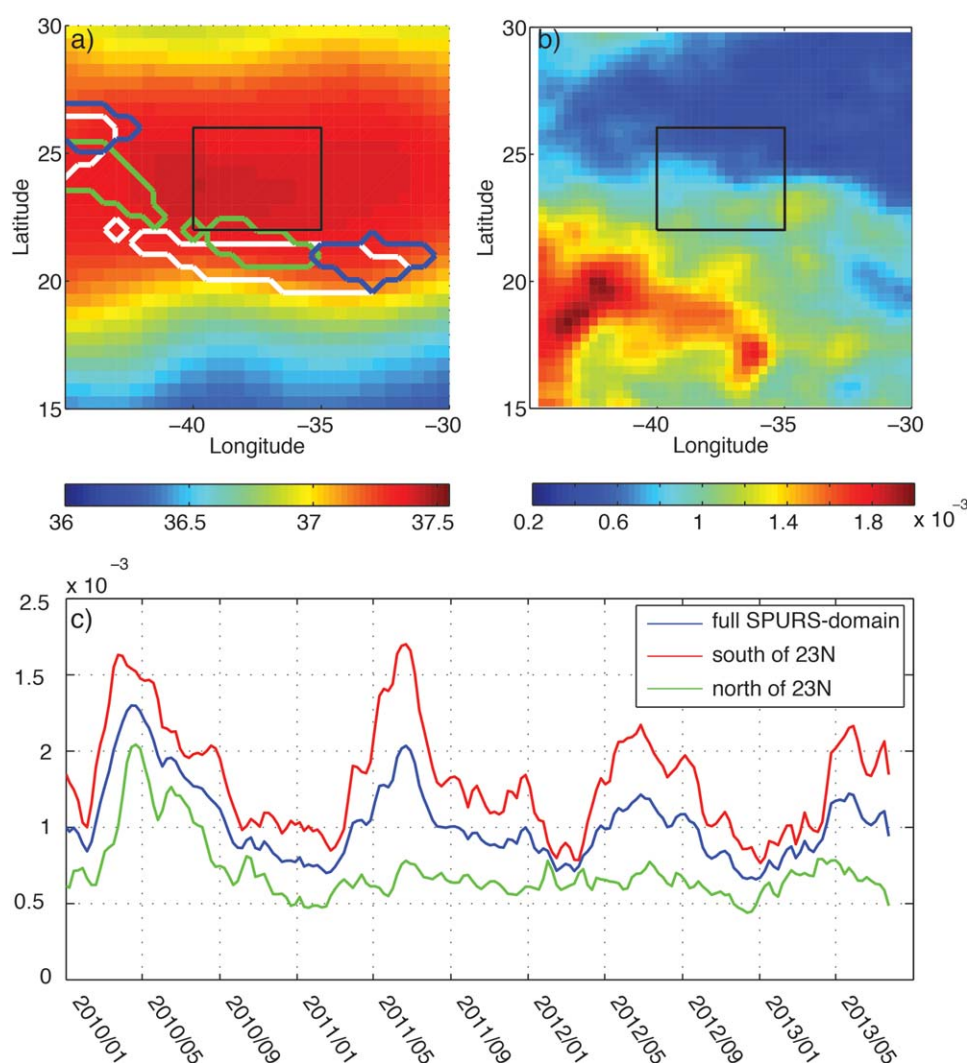
Figure 7. (a) Mixed layer salinity (PSU) in the SPURS-domain from MIMOC climatology averaged from February to April (months of the deepest mixed layers) in color. Contoured are different water masses from the T/S diagram in Figure 4: white: the approximate range of the S-max; blue and green: the T/S characteristics of the two fresh/warm features (survey 1 and 4 respectively) discovered during the SAR-MIENTO cruise. (b) Mean of EKE (m^2/s^2) from 2000 to 2013 in the SPURS-domain. Black box indicates CRUISE-domain. (c) Time series of EKE (m^2/s^2) in the SPURS-domain.

structures appear tightly associated with mesoscale dynamics. Scales of fresh and warm features are on the order of the first baroclinic Rossby radius within the region ($\sim 40-50$ km [*Chelton et al.*, 1998]), or larger (at least in the beginning of their evolution). Their movement is well explained by the geostrophic velocity anomalies, which agree well with the instantaneous velocities from the ship. While we are only evaluating two fresh and warm features here, the evidence for the role of mesoscale dynamics in the evolution of these features is compelling. When we consider mesoscale turbulence/eddy fluxes as a mechanism for the export of salinity out of the SSS-max to balance the net evaporation of the surface, it is important to mention that this does not just mean import of fresher water into the salty water, but at the same time an export of salty water out of the SSS-max is needed. Mesoscale turbulence exchanges salinity by stirring (and subsequently mixing) of waters along a background salinity gradient. To estimate the potential importance of turbulent salinity flux to the salinity budget in the mixed layer and the role in compensating the net evaporation, we approximate the turbulent fluxes following equation (8). We use the annual mean SSS field from the MIMOC climatology as the estimates of the salinity fields excluding the eddy effects. To obtain a reasonable estimate of the turbulent flux, it is important that the mean tracer field does not show signatures of the actual eddies, which would enhance the curvature of the field and artificially inflate the flux estimate. The MIMOC climatology seems useful in this context since it was specifically derived to minimize the
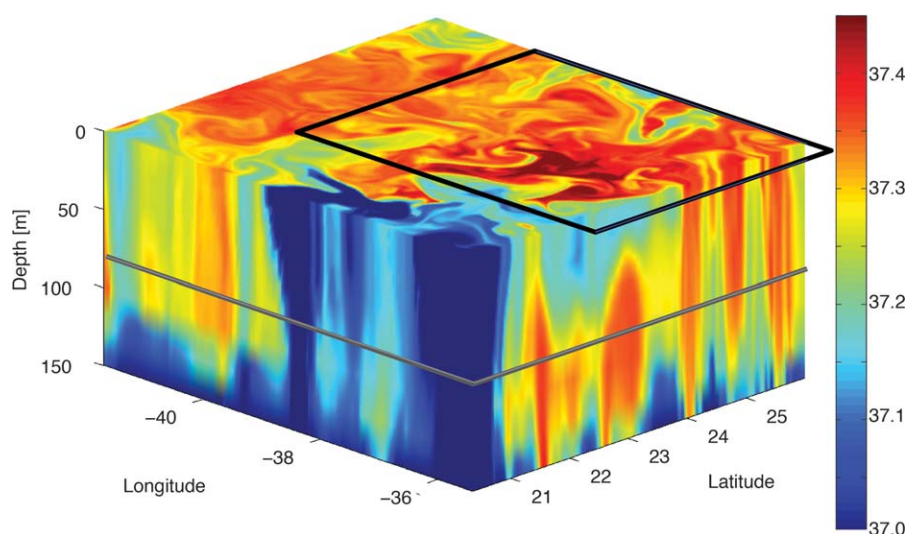
Figure 8. Shown in color is a sliced 3-D salinity (PSU) field from a ROMS simulation, showing a feature similar to the one seen in the Sea-Soar data (Figure 3). Gray line denotes a depth of 80 m. The black surface box marks the measurement domain shown in previous figures.

influence of transient structures like eddies in the climatological Argo fields. Furthermore visual inspection of the surface fields does not reveal any features of comparable size to the one investigated in this study. For simplicity, we restrict the estimate to a constant eddy diffusivity $K = 1000 - 3000 \ \frac{m^2}{s}$ from by [*Abernathey and Marshall*, 2013]. The part in square brackets of equation (8) thus can be written as: $[\nabla \cdot K \nabla \bar{S}] = [K \nabla^2 \bar{S}]$. A typical value for the research area (derived from MIMOC) is taken as $\nabla^2 \bar{S} = 2 \cdot 10^{-12} \ PSU/m^2$ combined with a mean mixed layer depth of $h = 50$ m and a reference salinity of $S_0 = 37.2 \ PSU$. This would result in a range of equivalent freshwater convergence of about 0.1–0.3 m/yr. Additionally, locally and seasonally the curvature of the salinity field can be considerably larger, meaning that this process can locally balance an even higher percentage of the net evaporation.

Future work has to be carried out to constrain these estimates and investigate the spatial and temporal distribution of the salinity divergence by geostrophic turbulence. Nonetheless, this result confirms that turbulent lateral fluxes are important in the annual salinity budget of the SSS-max, by compensating on average 10–30% of the mean annual net evaporation within the SPURS-domain, ($\sim$1 m/yr from [*Gordon and Giulivi*, 2014]). This result is in broad agreement with an independent study that investigates the direct turbulent flux estimates using SODA data and concludes that the turbulent fluxes might compensate more than 50% of the loss of freshwater through the surface [*Gordon and Giulivi*, 2014]. To relate the turbulent transport to the large-scale ocean and atmosphere context, one has to look at the surface properties of the Subtropical Atlantic region: a key difference between the northern and southern border of the SPURS-domain is the meridional density gradient. Either side shows strong gradients in salinity and temperature (Figure 1) but to the south both fields reinforce the density gradient, while in the north the effect on density is opposite. The salinity gradient supports a salinity flux out of the SSS-max region from both north and south, causing regular appearance of both cold and warm fresh features as seen during the SPURS cruise. Both features vary in their vertical structure and density anomaly with respect to the local climatology. The cold fresh features seem to have little variation with depth until the permanent mixed layer is reached and show generally a lower density difference to the surroundings than the warm features. The vertical structure of the latter suggests a higher baroclinicity due to the surface intensified temperature and salinity anomalies, which might explain the fast dispersal. The stronger climatological density gradient in the south might be favorable for the growth of baroclinic instabilities [*Charney*, 1947], which acting on a strong meridional salinity gradient cause eddy flux of salinity out of the SSS-max region, despite the low mean flow. Indeed the southwestern area exhibits stronger EKE than the rest of the SPURS-domain in the altimetry observations (Figure 7b). The EKE in this region furthermore shows a seasonal cycle with maxima in May–July and minima around January–March (Figure 7c). This general behavior is also seen in the ROMS model output. The net evaporation is anticorrelated to the surface salinity within the SPURS-domain [*Gordon and Giulivi*, 2014], whereas a

90-degree phase shift would be the expected relationship between net evaporation and surface salinity for a domain purely dominated by the surface forcing. This emphasizes the influence of oceanic processes in setting the surface characteristics in this region. The EKE peaks at about the same time as the surface salinity reaches its lowest point and the net evaporation is greatest, suggesting that the turbulent flux of freshwater might balance a major part of the net evaporation together with the mean Ekman flow of tropical waters toward the subtropics from the north and south and possibly vertical mixing at the base of the mixed layer. The variability in the EKE and turbulent flux on seasonal to interannual timescales is likely influenced by changes in the wind field. The influence of the wind field on the interannual salinity of the SSS-max was pointed out as early as the SSS-max was investigated [*Worthington*, 1976]. Idealized model studies show that eddy fluxes become important in the surface buoyancy transport in a downwelling regime like the subtropical gyres [*Cessi*, 2007].

It is important to realize that the Ekman flow and the eddy driven flux are coexisting processes and that the freshwater transport will be achieved as a combination of both. One notable difference between these two components might be the timescales of variability. The EKE shows a strong seasonal cycle and high interannual variability in both space and time, enabling it to play a role in the annual to interannual variability of the SSS-max waters, previously thought to be dominated by air sea fluxes only. Further work has to be carried out to investigate what process might link the large-scale wind field to the seasonal to interannual variability in turbulent fluxes. A likely candidate would be a change in large-scale density gradients by the Ekman transport/pumping, thus enhancing the available potential energy for baroclinic instabilities especially in the southern region.

A separate issue that needs discussion is the fast dispersal of the observed fresh and warm features in the center of the SSS-max domain. As stated earlier, the dominant process for the lateral movement of these features seems to be mesoscale dynamics, which set up strong mixed layer fronts. To add the water into the surrounding mixed layer, it ultimately has to be mixed vertically or laterally. Wind-driven mixing and vertical entrainment are a possible mechanism but would lead to a deepening of the mixed layer. No evidence for a significant deepening of the fresh mixed layer was recorded during the March 2013 cruise. Limitations of the SeaSoar coverage hinder a comprehensive comparison of the mixed layer depth during the evolution of the fresh warm patch. But CTD stations (Figure 3d, black diamonds) do not show any mixed layer deeper than when the feature was first sampled.

The scales of the strong lateral density front and low vertical stratification create an environment favorable for active submesoscale dynamics. Rossby numbers O(1)-O(10) [defined as $Ro = \zeta/f$, ζ is the relative vorticity and f the Coriolis parameter] and Richardson numbers O(1) are found frequently in the upper 50 meters. Given this environment, it is likely that active submesoscale dynamics drive strong mixing at the frontal edge and aid dispersal of the fresh water feature in a relatively short amount of time. Areas of strong density fronts along filaments and at the edges of eddies have been shown to contribute significantly to vertical exchanges in the upper ocean up to 500 m ([*Klein and Lapeyre*, 2009] give an overview of observational and numerical studies). *Mahadevan et al.* [2012] and *Fox-Kemper et al.* [2008] point out the importance of mixed layer eddies in restratifying the mixed layer. Wind mixing and restratification could work at the same time, and compete against each other [*Mahadevan et al.*, 2012]. Evidence for these mechanisms might be seen in the spreading and filamentation of the fresh/warm feature during its evolution, with little increase in depth during the process, as far as the measurements are able to identify the subsurface structure. To quantify the role of submesoscale dynamics in the dispersal of fresh water within the SSS-max domain is outside the scope of this study and should be evaluated in dedicated model studies since shipboard measurements barely resolve the largest feature ($\sim$ 10 km) in the submesoscale regime for the given stratification (typical scale is estimated as $L = Nd/f$ following [*Thomas et al.*, 2008], with N being the buoyancy frequency, f the Coriolis parameter, and d the depth of the mixed layer.) Above we pointed out the vertical freshwater columns at the leading edge of the fresh warm feature. Qualitatively the structure looks very similar to the upper ocean structure in other studies that focus on submesoscale frontal dynamics [*Fox-Kemper and Ferrari*, 2008; *Thomas et al.*, 2010], but at this point we are not able to attribute this structure explicitly to an ageostrophic circulation. Nonetheless, it seems plausible that submesoscale dynamics are active in this region and accelerate the dispersal as seen in the survey above. This would add a substantial part of the intruded freshwater to the mixed layer during the breakup, possibly even freshening deeper regions of low stratification above the permanent pycnocline but below the fresh feature and the associated fronts.

4.4. Implications for the Subtropical Cell

Salinity distributions in the North Atlantic suggest that the SSS-max water gets exported toward the southwest (Figure 4b) at a depth of about 100–150 m [*Worthington*, 1976]. Yet in the winter months (January/February/March), when the mixed layer is deepest the SSS-max water is too salty and cold to be connected to the S-max through isopycnal pathways. Diapycnal processes are thus needed to link the water properties in T/S space. This is confirmed in Figure 4a, using independent data from the MIMOC climatology. Since the used data record spans the period 2007–2011, it suggests that a diapycnal link is a general requirement and not an anomalous feature from the measurement period. The S-max in this study is not purely defined as south of the SPURS-domain but rather to the southwest, since the subsurface salinity maximum migrates toward the west with the North Equatorial Current (compare Figure 4b). The two fresh/warm features discussed above are similar as they provide a strong fresh/warm hence low density anomaly to the surrounding SSS-max waters. While the features differ slightly in their T/S characteristics, they both approach the properties of the S-max water and cross isopycnals (marker 1 and 9 in Figure 4c). Since we concluded earlier that a substantial amount of the anomalous water is added to the mixed layer by mixing processes, and that these fresh/warm events happen regularly, they are likely a necessary process that links the SSS-max to the S-max. The cold/fresh feature does not seem to contribute to setting the water properties toward the S-max, since they are denser than the SSS-max waters. This emphasizes the importance of mesoscale turbulence (specifically toward the south of the SSS-max) not only to the SSS-variability but also potentially to the properties of the subducted water in the lower limb of the STC. Further investigations of the variability in the lower limb and the role that mesoscale dynamics play in it are in preparation and outside of the scope of this study.

5. Conclusions

The observational data and model output presented in this paper suggest that the fresh and warm features, and their interaction with the SSS-max surface waters, represent the oceanic processes that ultimately balance a large part of the net evaporation in the subtropical Atlantic. Fresh and cold features seem to be abundant in both the observed data and the model output. The relative importance of these features to the freshwater input of the region remains speculative, since existing data do not enable us to estimate volume, evolution, and the timescale of dispersal for a large number of samples.

The observed fresh and warm features are not explicable by local rain, hence they must be advected from a different region. Intruding freshwater is quickly dispersed into the surrounding mixed layer and similar features are found frequently in ROMS model output and other data sets, confirming the importance for the salinity budget in the SSS-max region. Analyzing the scale and structure of the features, combined with the observed advection pattern, the equivalent freshwater flux is likely achieved by turbulent fluxes rather than mean flow within the mixed layer. The importance of these mesoscale dynamics to the lateral spreading of low salinity waters into the region is confirmed by the dominance of lateral scales larger than the first baroclinic Rossby radius and the good match between observed advection and geostrophic surface velocities from altimetry data. Fast dispersal is potentially caused by ageostrophic circulation at strong density fronts resulting from the advection of fresh and warm water into salty water. This would be consistent with a general picture of upper ocean turbulent fluxes, where mesoscale activity dominates lateral turbulent fluxes while vertical fluxes are dominated by mixed layer eddies and fronts [e.g., *Fox-Kemper et al.*, 2008].

Variable turbulent fluxes can provide a necessary input of freshwater into the SSS-max and consequently establish the connection between SSS-max and S-max in T/S space. This results in a high potential for variability in the water masses that replenish the S-max caused by a combination of variability in air sea fluxes [e.g., *Hurrell*, 1995; *Durack and Wijffels*, 2010] as well as mesoscale dynamics even on interannual timescales (while [*Curry et al.*, 2003] only considers the ocean dynamics to be important on decadal timescales). Indeed Aquarius L2 data show that the areas of highest interannual variability within the Aquarius record in the SPURS-domain are in the south and west of the CRUISE-domain (F. M. Bingham, in review, 2014), close to the areas of high EKE and where the surface properties match the S-max in the climatology. The EKE itself shows very high spatial and temporal variability over the course of 10 years. It is highly likely that the

interplay between these variations influences the transport of heat and freshwater through the STC, hence might have a significant influence on the global ocean circulation and climate.

How the mesoscale activity and turbulent flux of freshwater are controlled by large-scale atmospheric variables and linked to the S-max properties will be subject of future work.

References

Abernathey, R. P., and J. Marshall (2013), Global surface eddy diffusivities derived from satellite altimetry, *J. Geophys. Res. Oceans*, *118*, 901–916, doi:10.1002/jgrc.20066.

Blayo, E., and L. Debreu (1999), Adaptive mesh refinement for finite-difference ocean models: First experiments, *J. Phys. Oceanogr.*, *29*(6), 1239–1250.

Boccaletti, G., R. Ferrari, A. Adcroft, D. Ferreira, and J. Marshall (2005), The vertical structure of ocean heat transport, *Geophys. Res. Lett.*, *32*(10), L10603, doi:10.1029/2005GL022474.

Cessi, P. (2007), Regimes of thermocline scaling: The interaction of wind stress and surface buoyancy, *J. Phys. Oceanogr.*, *37*(8), 2009–2021. doi:10.1175/JPO3103.1.

Charney, J. G. (1947), The dynamics of long waves in a baroclinic westerly current, *J. Meteorol.*, *4*(5), 136–162.

Chelton, D. B., R. A. deSzoeke, M. G. Schlax, K. El Naggar, and N. Siwertz (1998), Geographical variability of the first baroclinic Rossby radius of deformation, *J. Phys. Oceanogr.*, *28*(3), 433–460.

Curry, R., B. Dickson, and I. Yashayaev (2003), A change in the freshwater balance of the Atlantic Ocean over the past four decades, *Nature*, *426*(6968), 826–829, doi:10.1038/nature02206.

Durack, P. J., and S. E. Wijffels (2010), Fifty-year trends in global ocean salinities and their relationship to broad-scale warming, *J. Clim.*, *23*(16), 4342–4362, doi:10.1175/2010JCLI3377.1.

Fairall, C. W., E. F. Bradley, D. P. Rogers, J. B. Edson, and G. S. Young (1996), Bulk parameterization of air-sea fluxes for Tropical Ocean-Global Atmosphere Coupled-Ocean Atmosphere Response Experiment, *J. Geophys. Res.*, *101*(C2), 3747–3764, doi:10.1029/95JC03205.

Font, J., A. Camps, A. Borges, M. Martín-Neira, J. Boutin, N. Reul, Y. H. Kerr, A. Hahne, and S. Mecklenburg (2010), SMOS: The challenging sea surface salinity measurement from space, *Proc. IEEE*, *98*(5), 649–665, doi:10.1109/JPROC.2009.2033096.

Fox-Kemper, B., and R. Ferrari (2008), Parameterization of mixed layer eddies, Part II: Prognosis and impact, *J. Phys. Oceanogr.*, *38*, 1166–1179, doi:10.1175/2007JPO3788.1.

Fox-Kemper, B., R. Ferrari, and R. Hallberg (2008), Parameterization of mixed layer eddies, Part I: Theory and diagnosis, *J. Phys. Oceanogr.*, *38*(6), 1145–1165, doi:10.1175/2007JPO3792.1.

Gordon, A., and C. Giulivi (2014), Ocean eddy freshwater flux convergence into the North Atlantic Subtropics, *J. Geophys. Res. Oceans*, *119*, doi:10.1002/2013JC009596, in press.

Hurrell, J. W. (1995), Decadal Trends in the North Atlantic Oscillation Regional Temperatures and Precipitation, *Science 269*(5224), 676–679, doi:10.1126/science.269.5224.676.

Klein, P., and G. Lapeyre (2009), The oceanic vertical pump induced by mesoscale and submesoscale turbulence, *Annu. Rev. Mar. Sci.*, *1*(1), 351–375, doi:10.1146/annurev.marine.010908.163704.

Lagerloef, G. (2013), Aquarius salinity validation analysis; data version 2.0, technical report, Aquarius SAC/D.

Mahadevan, A., E. D'Asaro, C. Lee, and M. J. Perry (2012), Eddy-driven stratification initiates north atlantic spring phytoplankton blooms, *Science*, *337*(6090), 54–58, doi:10.1126/science.1218740.

O'Connor, B. M., R. A. Fine, and D. B. Olson (2005), A global comparison of subtropical underwater formation rates, *Deep Sea Res., Part I* *52*(9), 1569–1590, doi:10.1016/j.dsr.2005.01.011.

Reverdin, G., E. Kestenare, C. Frankignoul, and T. Delcroix (2007), Surface salinity in the Atlantic Ocean (30S–50N), *Prog. Oceanogr.*, *73*(3-4), 311–340, doi:10.1016/j.pocean.2006.11.004.

Schanze, J. J., R. W. Schmitt, and L. L. Yu (2010), The global oceanic freshwater cycle: A state-of-the-art quantification, *J. Mar. Res.*, *68*(3), 569–595, doi:10.1357/002224010794657164.

Schmidtko, S., G. C. Johnson, and J. M. Lyman (2013), MIMOC: A global monthly isopycnal upper-ocean climatology with mixed layers, *J. Geophys. Res. Oceans*, *118*, 1658–1672, doi:10.1002/jgrc.20122.

Schmitt, R. W. (1995), The ocean component of the global water cycle, *Rev. Geophys.*, *33*(S2), 1395–1409.

Schmitt, R. W. (2008), Special issue on salinity, *Oceanography*, *21*(1), 20–29.

Schott, F. A., J. P. McCreary Jr., and G. C. Johnson (2004), Shallow overturning circulations of the tropical-subtropical oceans, in *Earth's Climate*, edited by C. Wang, S. P. Xie, and J. A. Carton, pp. 261–304, AGU, Washington, D. C.

Shchepetkin, A. F., and J. C. McWilliams (2009), Computational kernel algorithms for fine-scale, multi-process, long-time oceanic simulations, *Handbook of Numerical Analysis: Computational Methods for the Atmosphere and Oceans* 119.182 (2009):01202–0.

Thomas, L. N., A. Tandon, and A. Mahadevan (2008), Submesoscale processes and dynamics, in *Ocean Modeling in an Eddying Regime, Geophys. Monogr. Ser.*, edited by M. W. Hecht and H. Hasumi. pp. 17–38, AGU, Washington, D. C.

Thomas, L. N., C. M. Lee, and Y. Yoshikawa (2010), The subpolar front of the Japan/East Sea. Part II: Inverse method for determining the frontal vertical circulation, *J. Phys. Oceanogr.*, *40*(1), 3–25, doi:10.1175/2009JPO4018.1.

Worthington, L. V. (1976), On the north Atlantic circulation, *Johns Hopkins Oceanogr. Stud.*, *6*, 85–91.

BUSECKE ET AL.   4140